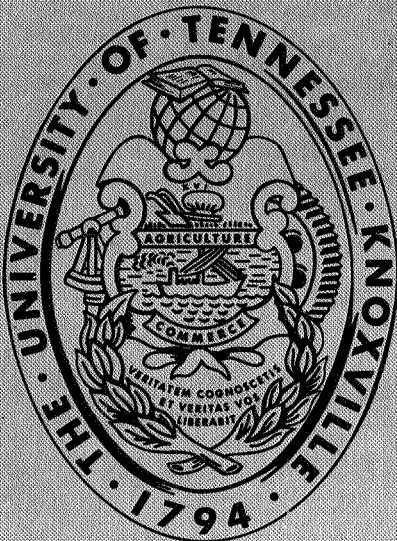


N 69 28386

NASA CR 101450



A MICHELSON INTERFEROMETER  
FOR DETECTING GRATING TABLE ROTATION

William L. Cole

**CASE FILE  
COPY**

May 1969

Work performed under N.A.S.A. Grants

~~NSG-630~~ and NGL 43-001-006

THE UNIVERSITY OF TENNESSEE  
Knoxville, Tennessee



A MICHELSON INTERFEROMETER FOR DETECTING  
GRATING TABLE ROTATION

---

A Thesis  
Presented to  
the Graduate Council of  
The University of Tennessee

---

In Partial Fulfillment  
of the Requirements for the Degree  
Master of Science

---

by  
William L. Cole  
June 1969

## ACKNOWLEDGMENTS

I would like to acknowledge the many persons who contributed to the completion of this work. I would like to thank Dr. John Garing for his suggestion which led to this work. The Master's committee was composed of Professors Norman M. Gailar, Robert J. Lovell, and Alvin H. Nielsen of the Physics Department of The University of Tennessee. It is a pleasure to express my deep appreciation to Dr. Gailar for his guidance in directing this work and to the other members of the examining committee for their advice.

I wish to especially thank W. J. Wiley for his many helpful discussions and his interest in this work.

The help of Ray Mink and other members of the Physics Department Instrument Shop is sincerely appreciated. The help of Glen Cunningham of the Physics Department Electronics Shop is certainly appreciated. Sincere thanks are due to Dr. Mack A. Breazeale for his helpful discussions and for the use of his laser.

The financial help given by The University of Tennessee by means of graduate and teaching assistantships is appreciated. This work was supported in part by the National Aeronautics and Space Administration under Research Grants NsG-539 and NGL-43-001-006.

I wish to thank my parents for all they have done to make this work possible. I also wish to thank my wife, Pat, for her understanding and encouragement throughout my graduate work.

## ABSTRACT

As better resolution in infrared spectroscopy becomes possible, more accurate measurement of line position is required. The technique to be described here involves a Michelson interferometer to detect angular motion of the grating table in an infrared spectrometer. The interferometer has been set up on the specially-supported concrete pad used to insulate the infrared spectrometer from external vibrations. The fringes were steady, when the substitute table was not rotating, although the spectrometer was not in operation. The variation in intensity of the central fringe will be used to provide markers on the same medium on which the spectrum is recorded. The markers will be closely spaced, and hopefully, they will be repeatable so they can be used as a reproducible scale for accurate measurement of line position. A brief review of the past and current techniques for measuring line position places this technique in proper perspective. The basic Michelson interferometer is discussed, and then the reader is led through the reasoning for the optical layout chosen. The possible sources of errors are discussed, and estimates are made for the amount of error necessary to affect the accuracy of wave number measurements of spectral line positions by  $0.001 \text{ cm}^{-1}$  using these markers. The optical alignment and specifications are given. Finally, suggestions are made concerning the setup and check-out of this interferometer.

## TABLE OF CONTENTS

CHAPTER	PAGE
I. REVIEW OF PAST AND CURRENT TECHNIQUES FOR MEASURING SPECTRAL LINE POSITION . . . . .	1
II. THIS TECHNIQUE FOR MEASURING SPECTRAL LINE POSITION . . . . .	5
III. BASIC MICHELSON INTERFEROMETER . . . . .	9
IV. DESIGN OF A MICHELSON INTERFEROMETER TO DETECT GRATING TABLE ROTATION . . . . .	15
V. EFFECT OF UNWANTED FRINGES ON THE PRECISION AND ACCURACY OF THIS TECHNIQUE . . . . .	21
VI. SOURCES OF UNWANTED FRINGE FORMATION . . . . .	26
Fluctuation of Ambient Air Pressure . . . . .	27
Fluctuation of Light Source Wavelength . . . . .	31
Fluctuation of Grating Table Temperature . . . . .	32
Fluctuation of Light Source Intensity . . . . .	34
Vibration of Optical Components . . . . .	35
VII. EFFECT OF IRREGULAR MOTION OF THE GRATING TABLE ON THE PRECISION AND ACCURACY OF THIS TECHNIQUE . . . . .	37
VIII. SYSTEMATIC EFFECTS ON THE SPACING OF THE MARKERS . . . . .	39
Variation of Optical Path in a Corner Cube with Angle of Incidence . . . . .	39
Sine Dependence of the Fringe Spacing . . . . .	43
IX. OPTICAL ALIGNMENT . . . . .	45

CHAPTER	PAGE
X. SPECIFICATIONS OF COMPONENTS . . . . .	51
XI. SUGGESTIONS . . . . .	54
BIBLIOGRAPHY . . . . .	58
VITA . . . . .	60

LIST OF TABLES

TABLE	PAGE
1. The Number of Unwanted Fringes as a Function of Angular Position of the Grating Table . . . . .	25
2. Temperature Change of Grating Table Necessary to Affect Precision of Line Position Measurement by $0.001 \text{ cm}^{-1}$ . . . .	33
3. The Number of Additional Fringes Caused by Misalignment of the Corner Cubes, for Various Angular Positions of the Grating Table . . . . .	42
4. The Number of Additional Fringes Caused by Misalignment of the Corner Cubes and by Not Having Identical Corner Cubes, for Various Angular Positions of the Grating Table . . . . .	42

## LIST OF FIGURES

FIGURE	PAGE
1. Optical Layout of the Basic Michelson Interferometer . . . . .	9
2. Formation of Circular Fringes in a Michelson Interferometer . . . . .	11
3. Formation of Localized Fringes in a Michelson Interferometer . . . . .	13
4. Detection of Grating Table Motion with a Plane Mirror . . . . .	15
5. Detection of Grating Table Motion Using a Corner Cube . . . . .	17
6. Optical Layout of the Michelson Interferometer Chosen to Detect Grating Table Motion . . . . .	19
7. Grating Table at an Angle $\theta$ From Its Zero Path Difference Position . . . . .	19
8. Angle at Which the Corner Cubes Leave the Beam . . . . .	20
9. Top View of the Optical Layout of the Michelson Interferometer . . . . .	46
10. Asymmetric Optical Layout . . . . .	48
11. Operational Circuit for the Detector . . . . .	52
12. Possible Future Optical Layout . . . . .	57



## CHAPTER I

### REVIEW OF PAST AND CURRENT TECHNIQUES FOR MEASURING SPECTRAL LINE POSITION

Extreme accuracy and precision in the measurement of line position were not important during the developmental period of infrared spectroscopy because of the poor resolution obtained. As improved optics and gratings gave better resolution, the measurement of line position became more critical. It is desirable for the measurement of  $\bar{\nu}$  to be ten times better than the resolution. Now that resolution of the order of  $0.01 \text{ cm}^{-1}$  appears possible, the line position should be measured to about  $0.001 \text{ cm}^{-1}$ . A brief review of the past and current techniques for measuring line position in the 1 to 25 micron range will place the author's technique in proper perspective.

During the early years of infrared spectroscopy the wave numbers of spectral lines were simply calculated from the grating equation  $\bar{\nu} = nK \csc \theta$ . where  $\bar{\nu}$  is the line position in wave numbers of a spectral line,  $n$  is the spectral order,  $K$  is an instrumental constant, and  $\theta$  is the angle between the positions of central image and the spectral line. The constant  $K$  depends on the spacing of the grating grooves and on the optical arrangement of the spectrometer. The constant  $K$  is determined by measuring the angles at which known spectral lines are observed. The angle  $\theta$  is obtained from a graduated circle upon which the grating rotates. This method does not yield very accurate results. The accuracy

to which the angle  $\theta$  can be measured is limited, and the constant  $K$  is not necessarily constant.

Another method involves recording known absorption or emission lines on either side of the unknown spectrum. Then a correlation is made between the known lines and their chart paper spacing so that interpolation will give the position of an unknown line. Of course the assumption must be made that the grating drive is not erratic.

The lack of smoothness in the rotational motion of the grating introduces error in the recorded spectrum. To reduce this error an interferometrically controlled hydraulic mirror drive was developed by Ameer and Benesch (1) for high precision scanning. The method gives good results but requires constant mechanical care and is limited in range.

Rank et al. (2, 3) use a wedge scanner with the grating at rest to scan accurately a small range in wave number. He uses an echelle grating to get closely-spaced absorption lines in high order which are recorded as wave number markers by the same chart recorder pen used in recording the unknown spectrum. It is important to have a standard line available for every  $8 \text{ cm}^{-1}$  interval, the range of the wedge scanner. Fiduciary markers obtained from the drive motor for the wedge scanner are used in determining the unknown line position from the standard line. Since the standard lines are not close enough together in some parts of the spectrum, intermediate markers by other means are required for these regions. The wedge scanner is very accurate but can only be used for a small range in wave number.

Three basic techniques exist which use a Fabry-Perot etalon. One method (4) involves varying the pressure of the gas between the etalon plates. The change in index of refraction causes a scan in wavelength. The scan is slow, however, and the range is extremely small. The system can be difficult to maintain in working order. The system is calibrated by scanning through known lines.

By displacing (5) one of the Fabry-Perot etalon plates parallel to itself the plate separation can be changed to give a scan in wavelength. When used in the far infrared, this method gives good resolution, limited by the maximum range over which the plate can be smoothly displaced. Progress has been made in the near infrared. The accuracy of this technique depends on the workmanship of the moving parts, and the Fabry-Perot etalons must be kept in proper alignment. This method requires access to a computer so that a Fourier transform can be performed on the recorded data. Good resolution becomes increasingly difficult closer to the near infrared. Some of the mechanical difficulties are removed by a technique (6) which replaces the translational motion of an etalon plate by a rotational motion, though the other disadvantages remain.

Another technique uses so-called Fabry-Perot channel fringes. In this method the index of refraction between the etalon plates and the etalon plate separation are constant. Visible light is passed through a prism to get a small range in wavelength. Then the light falls onto a Fabry-Perot etalon, and only certain wavelengths pass through. The light which gets through then falls on the grating. The motion of the grating brings these channel fringes in succession across a detector. The outputs



from the two detectors are put on separate pens of a chart recorder. This technique gives fringes equally spaced in wave number next to the unknown spectrum so that interpolation can be performed to find line positions. The absolute positions on this wave number scale are determined by recording suitable infrared standards on the pen normally used to record the unknown spectra and by recording the channel fringes on their usual pen. This method cannot put the known lines as close as desired. Also, sometimes either the known lines or the channel fringes, or both, cannot be obtained in the region desired. The temperature of the etalon must be kept constant. The etalon spacing must necessarily be quite small if the channel fringes are to be close enough together to serve as wave number markers. This problem is decreased if infrared light can be used with the etalon and if an appropriate detector for the infrared fringes is available.

Another method uses emission lines as wave number markers on a double pen recorder. The emission lines are recorded with known infrared lines on the other pen in order to use the emission lines for absolute measurements. The standards are not generally as close together as one would like to have them.

According to Garing (7) one group mounted one reflector of a Michelson interferometer on a nut that rode the screw driving the tangent arm. The interference fringes were used to put a mark on chart paper each time the grating moved through a small increment of angle and a fringe was formed. The writer is not acquainted with the results of this method or with the group.

## CHAPTER II

### THIS TECHNIQUE FOR MEASURING SPECTRAL LINE POSITION

The method described in this thesis for measuring spectral line position will use a Michelson interferometer to detect angular motion of the grating table. The light beam from a 6,328 Angstrom laser will be split by a beam splitter into two beams which are then directed to corner cube reflectors mounted on the grating table. Each split beam will make a double pass through its corner cube. Double-passing increases the sensitivity of the interferometer by increasing the path difference associated with any given position of the grating table. The split beams then return to the beam splitter where portions of the two beams combine and proceed to the detection system. As the grating table rotates, the optical path in one arm of the interferometer will shorten, and the optical path in the other arm will lengthen. If sources of unwanted fringe formation (to be discussed later) can be neglected, then fringes will form and disappear only when the grating table rotates. A fringe will be formed each time the table rotates through a small increment of angle. The size of this angular increment will depend on the angular position of the grating table. The variation in light intensity will be detected and will be used to put marker pips on chart paper or on magnetic tape. Thus the spacing of the associated marker pips will depend on the angular position of the table. Simultaneously, the unknown spectrum

will be recorded on the same chart paper or magnetic tape. These markers will come close enough so that interpolation between the markers will not be required. The spacing of the markers will correspond to a wave number interval ranging from 0.004 to  $0.0002 \text{ cm}^{-1}$ , the exact value depending on the position of the grating table and on the spectral region.

The markers may be used in one or more of several ways to determine the line positions of unknown spectral lines, assuming that sources of unwanted fringe formation can be neglected. More than one method may be used if a check is needed. Several possible methods of using the markers are now discussed.

In the first method, a scan is made to record known lines on either side of the unknown spectra. The marker pips are recorded simultaneously. If the range covered by the grating during the scan is small, then the spacing of the markers may not change appreciably. If so, linear interpolation will give the line positions of unknown spectral lines which lie between the known lines. For larger ranges in angle, the spacing of the markers may change appreciably. In such cases, some other type of curve fitting must be used. In all cases, the type of curve fitting required will be determined by the type of curve fitting that is needed to interpolate correctly the line position of a known line between two other known lines. The known lines used should lie in the range of angular position where the unknown spectrum will be recorded.

Another means of using the markers to determine line positions of unknown spectral lines requires an accurate means of measuring the angle through which the grating table turns. The relationship between a known



angular rotation and the number of marker spaces recorded is established. This relationship may be linear or may require more sophisticated curve fitting, depending on the range in angle. Next, a scan is made from a spectral line whose angular position and wavelength are known accurately over to the unknown spectra. The number of marker spaces from the known angular position to a specific unknown line are then converted to a change in angular position. The angular position of the unknown line is then found. Finally, the grating equation is used to find  $\bar{\nu}$ , the line position of the unknown spectral line, from the order of the unknown line, the angular position of the unknown line, and the grating constant. The calibration relationship should be determined from known lines recorded during the scan through the unknown spectra, since the calibration may change from one scan to the next. If the calibration does not change noticeably for long periods of time, then of course the calibration need only be checked periodically.

Still another method is to record channel fringes on one pen of the chart record while recording the marker pips with an event marker. Simultaneously, a scan is made to record one or more known spectral lines and the unknown spectra. The channel fringes will be spaced equally in wave number. The marker pips will be closer together than the channel fringes. The spacing of the marker pips should not change appreciably from one channel fringe to the next, but should only change over many channel fringes. Therefore, the marker pips can be used to interpolate, probably linearly, between any two channel fringes. The channel fringes

will provide a coarse scale and the marker pips a fine scale for determining the line position of an unknown spectral line from a known line.

The interferometer will be mounted inside the spectrometer vacuum tank so the temperature and index of refraction should be constant and reproducible. This method is limited in range to only several degrees of grating table motion, but this is quite acceptable. The limit will be set either by a maximum path difference allowed or by the fact that each corner cube begins to leave the beam from the beam splitter. The latter effect will determine the maximum range if large path differences are no problem. The method is not slow and should be dependable in operation and maintenance.

The interferometer has been set up on the specially-supported concrete pad used to insulate the infrared spectrometer from external vibrations. The fringes were steady when the substitute table was not rotating although the spectrometer was not in operation. The detector circuit was adjusted so that variations in the intensity of the central fringe were easily detected.

## CHAPTER III

### BASIC MICHELSON INTERFEROMETER

The basic Michelson interferometer consists of an extended source (S) of nearly monochromatic light, a beam splitter (BS), two plane front-surface mirrors ( $M_1$  and  $M_2$ ), and a detector (D) arranged as shown in Figure 1.

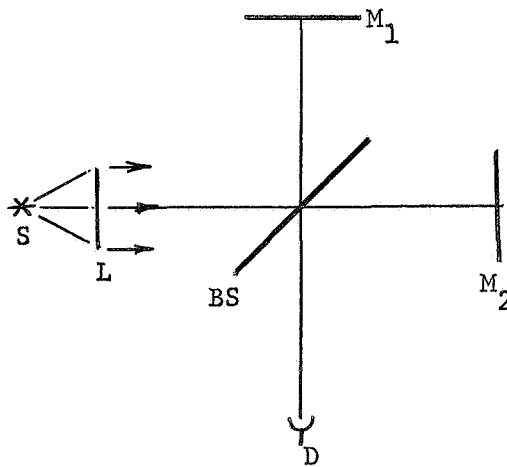


Figure 1. Optical layout of the basic Michelson interferometer.

A lens (L) is used if the source is not extended. The normals of the mirrors and beam splitters are horizontal. The mirrors are at right angles to each other, and the beam splitter makes a 45 degree angle with each of the mirrors. The light beam from the source is horizontal and makes a 45 degree angle of the incidence with the beam splitter.



Light falling on the beam splitter at any angle of incidence will be partially reflected and partially transmitted. If the beam is not split into two beams of equal intensity, then the difference in the intensity will constitute a steady background of light upon which fringes are viewed, and the contrast between the bright and dark fringes is reduced. Thus, it is important to make the split beams as close to being equally intense as possible. To do this the light beam from the source is directed at a 45 degree angle of incidence on the beam splitter. The beam splitter itself has an antireflection coating on one of its surfaces so that as much of the beam splitting as possible occurs at the other surface, called here the primary surface. The primary surface has a special coating so that transmission equals reflectance to within 2 to 3 percent. Absorption is only a fraction of a percent. Thus light from the source is separated into two beams (1 and 2) of about equal intensity. These beams are then reflected back toward the beam splitter by  $M_1$  and  $M_2$ . The portions of each beam which proceed from the beam splitter toward the detector interfere as long as the path difference is less than some maximum value which depends on the coherence length of the light.

Circular fringes are formed when  $M_1$  and  $M_2$  are exactly perpendicular to one another. Then the virtual image  $M_2'$  of  $M_2$  formed by reflection in the beam splitter will be parallel to  $M_1$ . Figure 2 shows the extended source (S), mirror ( $M_1$ ), and virtual mirror ( $M_2'$ ). Consider light from a source point P. Some of the light rays are reflected from  $M_1$  and some are reflected from  $M_2'$ . The reflected rays then proceed toward the detector (D), their parallel paths each making an angle  $\theta$  with a horizontal axis.

If  $d$  is the separation of  $M_1$  and  $M_2'$ , then the path difference between rays reflected from  $M_1$  and rays reflected from  $M_2'$  is  $2d \cos \theta$ . Constructive interference will occur when this path difference equals an integral multiple ( $m$ ) of the wavelength ( $\lambda$ ) of the light source:

$$2d \cos \theta = m \lambda. \quad (1)$$

For a given  $m$ ,  $\lambda$ , and  $d$ , the angle  $\theta$  must have a particular value. Therefore, the maxima form bright circles centered about the horizontal axis. Circular minima, specified by a similar relation, form dark circular rings which alternate with the bright ones.

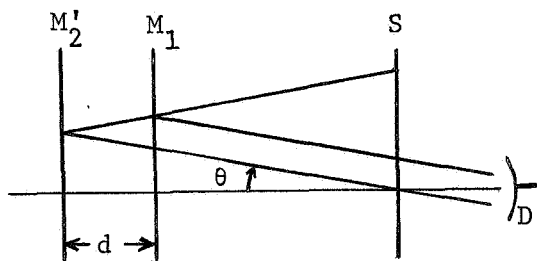


Figure 2. Formation of circular fringes in a Michelson interferometer.

The product  $m\lambda$  has a definite value for a particular fringe. Then, for a given fringe, equation (1) shows that  $\theta$  must change if  $d$  changes. If  $d$  decreases, then  $\theta$  must decrease so that  $\cos \theta$  will increase and the product  $2d \cos \theta$  will remain constant. Thus, the radius of each fringe will decrease as the path difference is decreased. All fringes will shrink, and the one with the smallest radius will disappear each time  $d$

decreases by one-half of a wavelength. The central fringe will be alternately bright and dark. The rings become more widely spaced as  $d$  decreases. At zero path difference, the whole field of view will be either dark or bright depending on whether the light beam which reflects in air at the beam splitter undergoes a phase change or not. If present, the phase change will be 180 degrees, which is equivalent to a path difference of one-half of a wavelength. If  $d$  is increased, then the circular fringes grow out of the center and the rings become more closely spaced. As  $d$  increases, the central fringe is alternately bright and dark.

Therefore, if one of the two plane mirrors is kept at rest and the other plane mirror is translated parallel to the direction of its normal, then the central fringe will go from bright to dark and back to bright as the mirror moves through a distance of one-half of a wavelength. This follows from the fact that at the center  $\cos \theta = 1$ , so that equation (1) becomes

$$2d = m \lambda. \quad (2)$$

If  $d$  changes by one-half of a wavelength, then  $m$  changes by unity.

If mirrors  $M_1$  and  $M_2$  are not exactly perpendicular, then what are termed as localized fringes will be seen. These fringes result mainly from path differences because the mirrors are not perpendicular. The plane mirror  $M_1$  and the virtual mirror  $M_2'$  are not parallel, as shown in Figure 3. The effect is quite similar to fringes formed by a wedge-shaped film. Localized fringes in a Michelson interferometer are slightly



curved because the path difference does vary slightly with angle. Localized fringes can be seen with monochromatic light only for small path differences, compared with the path differences over which circular fringes can be seen.

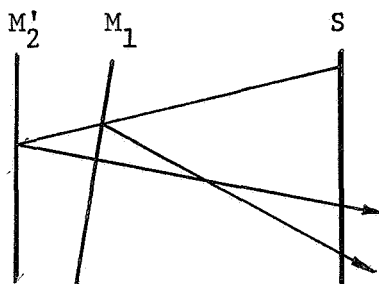


Figure 3. Formation of localized fringes in a Michelson interferometer.

The maximum path difference over which circular fringes are visible depends directly on the coherence length of the light. The coherence length is inversely proportional to the spread in wavelength of the source light. Thus the more nearly monochromatic a light source is, the longer is its coherence length.

If only a few distinct, close wavelengths are present, as in a laser which has only a few longitudinal modes excited, then the visibility of the fringes will alternately decrease and increase as path difference is increased. This phenomenon is similar to acoustical beats. The visibility refers to the difference in intensity between adjacent bright and dark fringes. The intensity of the minimum visibility will depend on the amplitudes of the wavelengths present. Consider the path difference

where one of the points of minimum visibility occurs. For some range of path difference on either side of this path difference it may be quite difficult or impossible to distinguish between bright and dark fringes. The degree of difficulty will depend on the detector sensitivity and on the magnitude of the minimum intensity. The useful range in path difference may be limited by the first occurrence of this minimum visibility on each side of zero path difference. If such visibility is a problem then a laser operating with only a single longitudinal mode should be used. The usable path difference will then be limited by the coherence length of the light and not by intermediate variations in the visibility.

## CHAPTER IV

### DESIGN OF A MICHELSON INTERFEROMETER TO DETECT GRATING TABLE ROTATION

Consider the problem of detecting grating motion by means of some sort of Michelson interferometric setup. The grating motion arises from the rotation of a table on which the grating is mounted. Suppose the flat mirror in one arm of the basic Michelson interferometer were mounted on the table (T) at one side of the grating (G), as shown in Figure 4. Then the rotational motion of the mirror would change the path difference, resulting in the formation and disappearance of fringes. These fringes

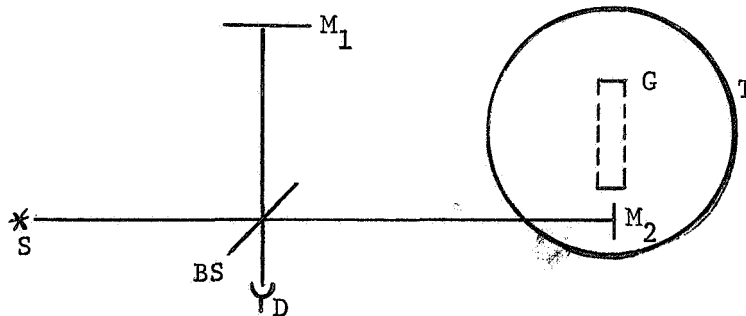


Figure 4. Detection of grating table motion with a plane mirror.

would, in fact, be localized fringes and would only be observed over a small range in angle. Recall that localized fringes are only visible over a small range in path difference. Another reason for the small useful range in path difference is the fact that, as  $M_2$  rotates with the grating table, optical alignment is lost.

These problems can be overcome by use of a retroreflector in place of mirror  $M_2$ . As the grating table rotates, a retroreflector will maintain the optical alignment, as long as the beam strikes it, of course. There are two basic types of retroreflectors: cat's eye reflectors and corner cube reflectors. A cat's eye reflector is not suggested because of the difficulty in maintaining the cat's eye itself in proper optical alignment. A corner cube is simply a corner cut off of a cubical piece of glass. The three mutually perpendicular faces are the reflecting surfaces for a beam of light which enters the diagonal face. The diagonal face is usually cut so that it makes equal angles with the three reflecting surfaces in order to provide maximum aperture. I will refer to the diagonal surface of a corner cube as its front surface. A corner cube, like the cat's eye retroreflector, has the property that it will return an incident beam of light parallel to the direction from which it came, regardless of the angle of incidence with a normal to the front surface. The accuracy with which a reflected beam is returned parallel to the incident beam depends on the accuracy of the 90 degree angles between the mutually perpendicular corner cube surfaces. Thus, a corner cube will maintain the desired optical alignment as the grating table rotates. Of course, the grating table can be rotated so far that the corner cube will begin to move out of the oncoming light from the beam splitter. As a result, less and less of the beam will be returned by the corner cube. The difference between the bright and dark fringes will decrease, and detector sensitivity will determine the maximum useful angle, assuming no other limiting conditions. At this maximum angle, just barely enough light is returned by the corner cube to establish detectable fringes.

A corner cube not only acts on an incoming beam so that the returning beam is parallel to the incident beam, but also so that the two beams are displaced from one another. This displacement would prevent the formation of fringes. This problem can be overcome, and the sensitivity of the interferometer can be increased at the same time by placing a plane front mirror ( $M_2$ ) in a position to return the displaced beam back through the corner cube (CC) for a second pass (see Figure 5).

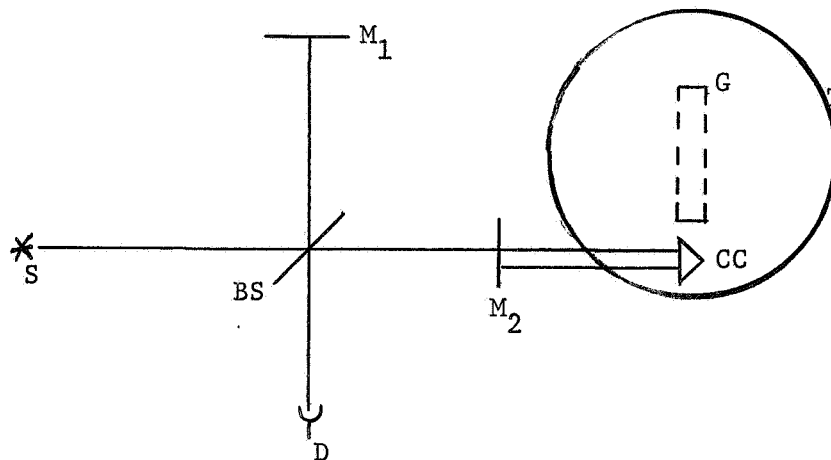


Figure 5. Detection of grating table motion using a corner cube.

The corner cube is positioned so that, at zero path difference, the displacement is in a vertical direction. In this position a horizontal beam of light from the beam splitter will pass over mirror  $M_2$  and fall on the corner cube (CC). The beam is displaced downward and heads toward  $M_2$ . The mirror  $M_2$  causes the light to retrace its path back through the corner cube and on to the beam splitter. This double pass through the corner cube serves to remove the displacement of the beam and also increases any path difference by a factor of two.

The next logical step is to modify the optical layout of a Michelson interferometer so that both arms of the interferometer involve a corner cube mounted on the grating table, one on each side of the grating. Each arm would use a plane front mirror to return the displaced beam back toward the corner cube for a second pass. Such an arrangement would be twice as sensitive as the arrangement shown in Figure 5. As the grating table rotates, the path length in one arm of the interferometer would increase and the path length in the other arm would decrease. A search of the literature on this field brought my attention to the work done by Marzolf (8) on an angle-measuring interferometer for use with an x-ray spectrometer. My optical layout (shown in Figure 6) is quite similar to his. The top views of the optical layout in Figures 5 and 6 show the beams entering and leaving each corner cube as being displaced horizontally from one another for clarity. Actually, for the zero path difference position, the beams will be displaced only vertically from each other, as pointed out above.

Referring to Figure 7, it can be seen that when the grating table is at an angle  $\theta$  from its zero path difference position, the path difference is given by  $8r \sin \theta$ , where  $r$  is equal to the radial distance from the center of the grating table to the center of each corner cube. Of course, the maximum path difference occurs when the grating table is at the maximum angle from its zero path difference position.

Assuming that a path difference of about 100 centimeters is no problem, then the maximum range in angle of the grating table is determined by the angle at which the corner cubes start to leave the light beams from



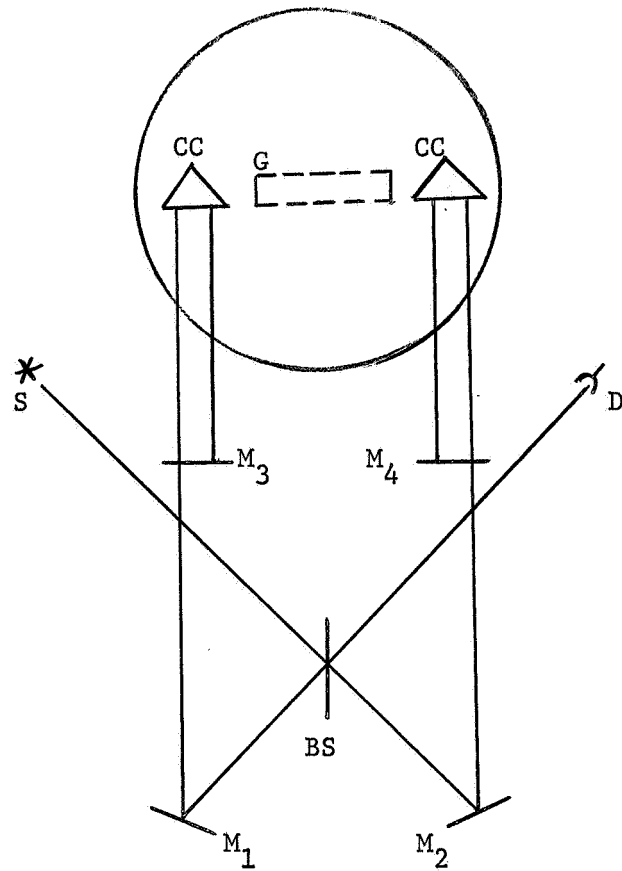


Figure 6. Optical layout of the Michelson interferometer chosen to detect grating table motion.

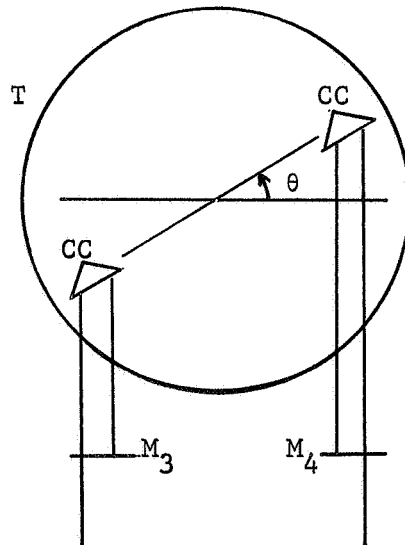


Figure 7. Grating table at an angle  $\theta$  from its zero path difference position.

the beam splitter. An estimate of this maximum angle is determined from geometric considerations based on the aperture size of the corner cubes and on their radial positions. The estimate is made with the following assumptions: each corner cube has a 2.5 centimeter aperture, the corner cubes are each at a radial distance of 25 centimeters, and the source beam is expanded to a diameter of 2.5 centimeters. Figure 8 shows that the maximum angle is determined by

$$\cos \theta = \frac{23.75}{26.25}$$

$$\theta \approx 25^\circ.$$

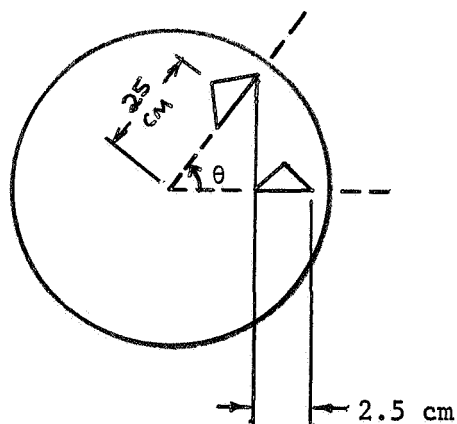


Figure 8. Angle at which the corner cubes leave the beam.

## CHAPTER V

### EFFECT OF UNWANTED FRINGES ON THE PRECISION AND ACCURACY OF THIS TECHNIQUE

Any fringe motion which is not due to motion of the grating table is not wanted. Unwanted fringes will be interpreted as a corresponding scan through the spectral region. Hopefully, each marker will be accurate within  $0.001 \text{ cm}^{-1}$ . An accuracy of  $0.001 \text{ cm}^{-1}$  will require that the number of unwanted fringes be less than a certain number. The number of unwanted fringes corresponding to  $0.001 \text{ cm}^{-1}$  will depend on the angular position of the grating and the line positions in wave numbers of the spectral lines studied at that angular position. Estimates of this number of unwanted fringes are made for four different angular positions of the grating table. The equation used for making these estimates is derived now. The grating equation is

$$\bar{\nu} = n K \csc \phi \quad (3)$$

where  $\bar{\nu}$  is the line position in wave numbers of a spectral line observed in  $n$ th order at angle  $\phi$  measured from central image using a grating with an associated constant  $K$ . Taking the differential of both sides of equation (3), assuming  $n$  and  $K$  are constant, gives

$$d\bar{\nu} = \frac{n K \cos \phi d\phi}{\sin^2 \phi} . \quad (4)$$

A negative sign from the differential of  $\csc \theta$  is omitted because it does not affect these considerations. Using equation (3), equation (4) can be put in the form:

$$d\bar{v} = \bar{v} \cot \phi d\phi. \quad (5)$$

Replacing the differentials in equation (5) with small increments, using the delta notation, gives

$$\Delta\bar{v} = 2 \bar{v} \cot \phi \Delta\phi. \quad (6)$$

A factor of two is included in equation (6) which does not come from equation (5). This factor of two is needed because the entrance and exit slits are fixed in position and the grating rotation produces the scan. Both the angle of incidence and the angle of observation are measured from the normal to the grating. Therefore, both angles are changed as the grating rotates. Equation (3) was written assuming the angle of incidence was always 90 degrees.

The path difference (pd) for the interferometer shown in Figure 6, page 19, is given by

$$(pd) = 8r \sin \theta, \quad (7)$$

where  $r$  is the radial distance to each of the corner cubes and  $\theta$  is the angular position of the grating table with respect to its zero path difference position. Taking the differential of both sides of equation (7) and then replacing the differentials with small increments in the delta notation gives

$$\Delta(pd) = 8r \cos \theta \Delta\theta, \quad (8)$$

were  $r$  is assumed to be constant. The angles  $\theta$  and  $\phi$  are directly related because they both give the angular position of the grating table. Thus, if  $\theta$  changes by certain amount, then  $\phi$  must change by exactly the same amount. Therefore,  $\Delta\phi = \Delta\theta$ . Using this fact, equations (6) and (8) can be combined to give

$$\Delta(\text{pd}) = \frac{8r \cos \theta \Delta\bar{\nu}}{2\bar{\nu} \cot \phi}, \quad (9)$$

which can be written

$$\Delta(\text{pd}) = \frac{4r \cos \theta \tan \phi \Delta\bar{\nu}}{\bar{\nu}}, \quad (10)$$

since the reciprocal of  $\cot \phi$  is  $\tan \phi$ . The number of fringes or fractions of a fringe (represented in either case by  $F$ ) which are formed during a change in path difference is given by

$$F = \frac{\Delta(\text{pd})}{\lambda}, \quad (11)$$

where  $\lambda$  is the wavelength of the source light in the interferometer. The numerator and denominator must be in the same units of length, of course. Equation (10) can be used in equation (11) to give

$$F = \frac{4r \cos \theta \tan \phi \Delta\bar{\nu}}{\lambda \bar{\nu}}. \quad (12)$$

Note that the  $\lambda$  and  $\bar{\nu}$  in equation (12) are not related at all.  $\lambda$  is the wavelength of the source light used in the interferometer, and  $\bar{\nu}$  is the reciprocal of the wavelength of the spectral line being studied in the infrared spectrometer when the grating is at an angle  $\phi$  from central image. Equation (12) can be used to estimate the number of fringes associated with a scan through  $0.001 \text{ cm}^{-1}$  by the grating spectrometer.

Four estimates are made--for values of  $\theta$  equal to 2.5, 5, 10, and 20 degrees.  $\Delta\bar{\nu}$  is taken to be  $0.001 \text{ cm}^{-1}$  in each case. The angle of 2.5 degrees will be the most important range in angle because of the application for which the interferometer is intended. The fringes will be used to provide closely spaced markers for unknown spectra studied with an infrared spectrometer. The most critical range in angle over which the markers are needed is 2.5 degrees on either side of the zero path difference position of the grating table. The angle of 20 degrees represents the angle at which each corner cube will begin to move out of the light beam coming from the beam splitter. The value of  $r$  is taken to be 25 cm. in each case. The value of  $\phi$  changes as the value of  $\theta$  changes, as pointed out in the derivation of equation (9). When  $\theta$  is zero, then  $\phi$  is 63.5 degrees, the blaze angle for the grating to be used. The value of 2.5 degrees for  $\theta$  occurs on either side of the zero path difference position of the grating table. Thus  $\phi$  is either 61 or 66 degrees. The same considerations will apply for the other values of  $\theta$  used in the estimate. In each case both the larger and the smaller values of  $\phi$  were used. Thus, two estimates are obtained for each value of  $\theta$ . The results of the estimates are shown in Table 1 along with the values of  $\theta$ ,  $\phi$ , and  $\bar{\nu}$  used in each case. The values of  $\bar{\nu}$  used are values which represent, within an order of magnitude, the spectral regions typically studied at that position of the grating. The most demanding situation, both for the spectrometer and for the interferometer, will occur for small values of  $\theta$ . The spectrometer resolution will be best within a range of 2.5 degrees on either side of the blaze. Therefore, the measurement of line position



must be more accurate within this range of grating table position. The estimate of  $F$  shown in Table 1 for 2.5 degrees represents the most stringent control of unwanted fringe formation that will be required. The value of used is  $6.3 \times 10^{-5}$  centimeters, which is the wavelength of the laser to be used rounded to two significant digits.

TABLE 1  
THE NUMBER OF UNWANTED FRINGES AS A FUNCTION  
OF ANGULAR POSITION OF THE GRATING TABLE

$\theta$ , degrees	$\phi$ , degrees	$\bar{\nu}$ , $\text{cm}^{-1} \times 10^2$	$F$ , fringes
2.5	61.0	100	.28
2.5	66.0	100	.36
5	58.5	10	2.5
5	68.5	10	4.0
10	53.5	5	4.2
10	73.5	5	10
20	43.5	2.5	5.5
20	83.5	2.5	52

## CHAPTER VI

### SOURCES OF UNWANTED FRINGE FORMATION

Ideally the variation in the light intensity of the central fringe should correspond only to the motion of the grating table. Nevertheless, the central fringe can vary in intensity for other reasons. For example, for reasons discussed below, the grating table could be at rest, but the fringe detector would seem to indicate that the table is moving. Of course, this additional fringe motion will, if present, be added to fringe motion when the grating table is moving. Each of the sources for this unwanted fringe formation is discussed next. In several of the cases an estimate is made of how closely that source must be controlled so that the unwanted fringes formed will not correspond to more than  $0.001 \text{ cm}^{-1}$ . The limit of  $0.001 \text{ cm}^{-1}$  was chosen because a resolution of  $0.01 \text{ cm}^{-1}$  is hoped for in the spectral region where resolution is expected to be best. The number of unwanted fringes (to be designated in these discussions by  $F$ ) corresponding to  $0.001 \text{ cm}^{-1}$  will depend on the angular position of the grating table, on the grating itself, and on the line positions in wave numbers of the spectral lines studied at that angular position. When the grating table is at 2.5 degrees from its zero path difference position, about one-fourth of a fringe corresponds to a scan through  $0.001 \text{ cm}^{-1}$ . At 20 degrees about 10 fringes corresponds to  $0.001 \text{ cm}^{-1}$ . The equation (equation (12)) used to get these values and

the values for other positions of the grating table was developed in Chapter V. The wavelength of the monochromatic source is taken to be 6,328 Angstroms, and the radial distance from the center of the grating table to each corner cube is taken to be 25 centimeters.

#### I. FLUCTUATION OF AMBIENT AIR PRESSURE

The wavelength of light in a gas depends on the refractive index of the gas which in turn varies linearly with the gas pressure. Therefore, if the gas pressure in the interferometer environment changes, then the wavelength will change. Suppose the grating table is at rest so the path difference is constant. Equation (1) was written assuming the interferometer was in a vacuum. Actually the optical path difference (refractive index times the path difference) is equal to an integral multiple of the wavelength:

$$n \times (\text{path difference}) = m\lambda. \quad (13)$$

where the path difference is  $2d \cos \theta$ , and where  $n$  is the refractive index. Equation (13) shows that if the refractive index changes (which also changes  $\lambda$ ), then  $m$  will change. This means that as the pressure of the gas surrounding the interferometer changes, the central fringe will alternate between bright and dark. The effect is worse at greater path difference because a slight change in wavelength will accumulate over a distance of many wavelengths.

As estimate of how close the gas pressure must be controlled can be made as follows. Suppose the optical path difference is equal to an integral multiple  $m$  of the wavelength  $\lambda$  for a gas with refractive index

n. Equation (13) applies exactly to this situation. Now suppose the gas pressure changes to a new value so that F fringes are formed. Then m changes to m + F. Let n' denote the new refractive index and  $\lambda'$  the new wavelength. Then

$$n' \text{ (path difference)} = (m + F)\lambda. \quad (14)$$

The path difference is constant so equations (13) and (14) can be combined to give

$$\frac{m\lambda}{n} = \frac{(m + F)\lambda'}{n'}. \quad (15)$$

It is easily shown that

$$\frac{\lambda}{\lambda'} = \frac{n'}{n}. \quad (16)$$

Therefore equation (16) can be used to put equation (15) in the form:

$$\left(\frac{n'}{n}\right)^2 = 1 + \frac{F}{m}. \quad (17)$$

The value of m is given by

$$m = \frac{\text{path difference}}{\lambda} \quad (18)$$

to a good approximation since n is nearly one for air.

The estimate is made for two different values of maximum path difference--one corresponding to an angle of 2.5 degrees from zero path difference position and the other to an angle of 20 degrees. The estimate in each case was made as follows: The initial gas pressure was taken to be zero; that is, the interferometer was assumed to be in a perfect vacuum. Thus n equals one. Equation (18) was used to calculate the value of m. The values of m, n, and F were then used in equation (17) to get a

value of  $n'$ . The binomial expansion was used to get the square root of  $1 + \frac{F}{m}$  because  $m$  was a large number compared to  $F$  in each case. Then a proportion was set up using the fact that the refractive index of air at  $0^\circ\text{C}$  is equal to 1.000293 for a gas pressure of 760 millimeters and is equal exactly to one for a gas pressure of exactly zero.

As an example, consider the case where the angle is 2.5 degrees. The path difference is found first, as follows:

$$\begin{aligned} \text{path difference} &= 8r \sin \theta \\ &= (8) (25) \sin 2.5^\circ \\ &= 8.7 \text{ cm.} \end{aligned}$$

The value of path difference is given to the nearest tenth of a centimeter. Next, equation (18) is used to find  $m$  to two significant digits:

$$\begin{aligned} m &= \frac{\text{path difference}}{\lambda} \\ &= \frac{8.7}{6.3 \times 10^{-5}} \\ &= 1.4 \times 10^5, \end{aligned}$$

where the wavelength, 6,328 Angstroms, is expressed in centimeters and rounded to two significant digits. Now equation (17) is used to get  $n'$ , with  $n$  chosen to be one, for the reasons given above. The value of  $F$  at 2.5 degrees is one-fourth.

$$\begin{aligned} \left(\frac{n'}{n}\right)^2 &= 1 + \frac{1}{4m} \\ &= 1 + \frac{1}{4(1.4 \times 10^5)} \\ &= 1 + 1.8 \times 10^{-6} . \end{aligned}$$

Therefore,

$$n' = (1 + 1.8 \times 10^{-6})^{1/2}.$$

The binomial expansion through only the second term gives, to a good approximation,

$$n = 1.0000009.$$

The pressure associated with this refractive index can be found by linear interpolation with the values of air pressure and refractive index shown below.

p, Torr	n
0	1
p	1.0000009
760	1.000293

The value of p, rounded to two significant digits, is 2.4 Torr.

The results of the calculations indicate that the gas pressure fluctuations must be kept within a range of 2.4 Torr if the grating table is at 2.5 degrees. Similar calculations show that the gas pressure fluctuations must be kept within a range of 6.5 Torr if the grating table is at 20 degrees. The interferometer is to be located in a tank which is to be kept at a pressure on the order of microns. The pressure should certainly not change sufficiently to cause enough unwanted fringes to form to be equivalent to  $0.001 \text{ cm}^{-1}$ , and therefore, this source of unwanted fringe motion should not be a problem.



## II. FLUCTUATION OF LIGHT SOURCE WAVELENGTH

If the wavelength of the source changes, then the intensity of the central fringe will change, just as if the path difference were changing. The number of unwanted fringes will be greater at longer path differences. To estimate how closely the wavelength must be controlled, the change in wavelength necessary to form enough unwanted fringes (designated by  $F$ ) to correspond to  $0.001 \text{ cm}^{-1}$  is found. In this estimate the refractive index is considered to be constant and equal to one. The path difference is taken to be constant and equal to some maximum value. Then,

$$\text{path difference} = \text{constant} = m\lambda = (m + F)\lambda', \quad (19)$$

where  $m$  is an integer,  $\lambda$  is the original wavelength,  $\lambda'$  is the new wavelength, and  $F$  is the number of unwanted wavelengths. Let  $\Delta\lambda$  represent the change in wavelength so that  $\lambda' = \lambda - \Delta\lambda$ . Then,

$$m\lambda = (m + F)(\lambda - \Delta\lambda). \quad (20)$$

Using the fact that  $m$  is large compared to  $F$  and  $\Delta\lambda$  is small compared to  $\lambda$ , equation (20) can be simplified to give

$$\Delta\lambda = \frac{F\lambda}{m}, \quad (21)$$

where  $m$  is found from equation (18). Using equations (18) and (21) it is seen that the wavelength must be kept within 0.011 Angstroms for the grating table at 2.5 degrees from its zero path difference position. At 20 degrees the wavelength must be kept within 0.029 Angstroms. The frequency of 6,328 Angstrom wavelength light is  $4.74 \times 10^{14}$  cycles per second. Therefore, to control the wavelength within 0.011 Angstroms, for

example, will require the frequency to be controlled within 820 megacycles per second. A single frequency helium-neon laser will operate at 6.328 Angstroms within a range of 1,500 megacycles per second about its frequency of  $4.74 \times 10^{14}$  cycles per second if its frequency is not controlled. Commercially available, 6,328 Angstrom, single-frequency lasers with frequency control will keep the frequency within 100 megacycles or less. One commercially available laser will keep the frequency within  $\pm 1$  megacycle per day.

### III. FLUCTUATION OF GRATING TABLE TEMPERATURE

A change in temperature of the grating table will change the radial position of each corner cube. If the grating table is an angle  $\theta$  with respect to its zero path difference position, then a change of  $\Delta r$  in the radial position of each corner cube will move one corner cube closer to the beam splitter and the other further away. Considering the fact that the light beam in each arm of the interferometer passes through its corner cube twice, the change in path difference,  $\Delta(\text{pd})$ , will be

$$\Delta(\text{pd}) = 8 \Delta r \sin \theta. \quad (22)$$

If  $\alpha$  is the temperature coefficient of linear expansion and  $\Delta T$  is the temperature change, then

$$\Delta r = \alpha r \Delta T. \quad (23)$$

Therefore, the change in path difference associated with a change  $\Delta T$  in the temperature of the grating table is given by

$$\Delta(\text{pd}) = 8 \alpha r \sin \theta \Delta T. \quad (24)$$

If the number of unwanted fringes formed is not to exceed  $F$ , then

$$F\lambda = 8\alpha r \sin \theta \Delta T. \quad (25)$$

Note that the change in path difference is greatest when  $\theta$  has its maximum value, assuming all the other quantities are held constant, of course.

The estimate was made for two values of angles (2.5 degrees and 20 degrees) and two values of  $\alpha$  (for aluminum,  $\alpha$  is  $7.2 \times 10^{-5} (\text{C}^\circ)^{-1}$  and for invar,  $\alpha$  is  $0.27 \times 10^{-5} (\text{C}^\circ)^{-1}$ ). The results are shown in Table 2. The value of  $F$  was taken to be one-fourth at 2.5 degrees and 10 at 20 degrees.

TABLE 2  
TEMPERATURE CHANGE OF GRATING TABLE NECESSARY TO AFFECT  
PRECISION OF LINE POSITION MEASUREMENT BY  $0.001 \text{ CM}^{-1}$

$\alpha$ $(\text{C}^\circ)^{-1} \times 10^{-5}$	$\theta$ degrees	$\Delta T$ $\text{C}^\circ$
7.2	2.5	0.025
7.2	20	0.12
0.27	2.5	0.65
0.27	20	3.5

The results indicate that the corner cubes should be mounted on invar if the temperature fluctuates in short intervals of time over a range of  $0.025 \text{ C}^\circ$  at a grating position of 2.5 degrees from the zero path difference position.

The limits to which the gas pressure, the wavelength, and the temperature must each be controlled represent how closely they must be controlled over any short interval of time (short compared to the scan time of the unknown spectrum). The limits may be exceeded over a long period of time.

#### IV. FLUCTUATION OF LIGHT SOURCE INTENSITY

Still another random source of unwanted fringes is variation in intensity of the light source. Such variation will be interpreted by the fringe detector as variation in fringe intensity. If the source intensity fluctuates with a noticeable amplitude compared to the amplitude of the variation in fringe intensity associated with change in path difference, then an effort should be made to control the source intensity. Suppose this control is not possible, or is limited in its effectiveness. One possible way to eliminate this error would be to monitor the intensity with a detector looking at a portion of the beam taken out before the beam strikes the interferometer beam splitter. The output could be on the same chart paper on which the spectrum and the marker pips are recorded. Then when the source intensity varied too much, the corresponding spectral region could be run again, hopefully when the source intensity is more stable. If running three pens on the chart paper is not practical, then perhaps the output of the detector which is looking at the source intensity could be coupled with some sort of alarm system. Such an alarm system would be triggered when the detector output exceeded predetermined limits. It would be best if such a detector were actually

triggered only when the rate of change of the source detector exceeded some maximum value. Alternately, the output of the detector which monitors the source intensity might be used to adjust the source intensity as it drifts.

## V. VIBRATION OF OPTICAL COMPONENTS

Another random source of unwanted fringes is vibration of the mirrors, beam splitter, and corner cubes. Such vibration changes the path difference, and thus produces unwanted fringes. The size of the effect depends on the amplitude and frequency of the vibration. (As the amplitude and frequency increase, the path difference produced by the vibration increases.) As pointed out previously, the spectrometer in which the interferometer is to be placed is specially mounted to insulate the spectrometer from external vibration. Thus, external vibration will, hopefully, not be a problem. Internal vibration generated from such sources as the grating drive mechanism may be a problem, but again, hopefully not. If internal vibration is a problem, then the optical components should be specially mounted to insulate them from the vibration.

Fluctuation of the ambient air pressure, vibration of the optical components, fluctuation of source intensity, fluctuation in the wavelength of the source light, and the fluctuation of the temperature of the grating table are each random sources of unwanted fringe formation. Only random errors are important to control. Random errors will degrade the value of the markers because a given marker will not correspond exactly to the same position of the grating from one scan to the next. Any systematic

errors will affect the fringe spacing, and thus the associated marker spacing, in the same way from one scan to the next. Repeatable errors in the marker spacing do not affect the value of the markers for the purpose for which they are intended, if the repeatable errors are known to exist.

## CHAPTER VII

### EFFECT OF IRREGULAR MOTION OF THE GRATING TABLE ON THE PRECISION AND ACCURACY OF THIS TECHNIQUE

Irregular motion of the grating table will not affect the precision of the markers except possibly in two cases: momentary backward motion of the grating table and stick-slip of the grating table. If the grating table momentarily backs up for some reason, such as vibration, then the marker pips will form as the grating moves backward. At the same time the spectral region will be scanned in reverse also. If the momentary backward motion is not recognized by the experimenter, then additional fringes will change the number of wave numbers associated with the marker spacing, which in turn degrades the precision of the markers. As a result, the line positions of unknown spectral lines will not be interpreted correctly.

The detection of the direction of fringe motion will be necessary if the grating table is suspected of momentary backward motion. Momentary backward motion cannot be detected by the interferometer as it is now designed (see Figure 6, page 19). A single detector can only indicate that fringes are forming and disappearing. However, a method is available to detect the direction of the fringe motion. This method requires the beam (after interference) be split into two beams. These two beams then fall on separate detectors placed in the central fringe of each beam.



The two beams are made 90 degrees out of phase by some means, such as a phase retard plate. The signals from the detectors will then be 90 degrees out of phase--exactly the necessary input for electrical circuits designed to perform reversible counting. The circuits used to perform reversible counting might be modified since it is unnecessary to count the fringes but only to watch for their occurrence. The detection of the direction of fringe motion has not been performed or investigated in detail by me. Marzolf counted fringes reversibly. Cook and Marzetta (10) discuss reversible fringe counting, as do Peck and Obetz (11).

If the grating table experiences stick-slip, then the marker pips will not be recorded at their usual interval on the chart paper or on the magnetic tape. The fringe detector and the spectral detectors will follow the motion if their response times are short enough. The chart paper or magnetic tape will continue to move in the same direction. During the slip phase of the motion, the grating table will move faster than it normally is driven. Thus, the spectral scan will be faster than normal during the slip phase. At first it might be supposed that stick-slip will definitely affect the precision of the markers. This is not so, however, since the markers will still correspond to the same point in the spectrum if both detectors can follow the motion. The momentary halt of the grating table during the stick-slip stops both the formation of the fringes and the scan of the spectral region. When the table begins to move again, then both the fringe formation and the spectral scan start again also. If either the fringe detector or the spectral detector does not have a short response time, then stick-slip or vibration may provide a rapid change in intensity which cannot be properly followed by that detector.

## CHAPTER VIII

### SYSTEMATIC EFFECTS ON THE SPACING OF THE MARKERS

#### I. VARIATION OF OPTICAL PATH IN A CORNER

##### CUBE WITH ANGLE OF INCIDENCE

One systematic effect on the spacing of the markers is due to the use of corner cubes as reflectors. The optical path length in glass of a ray passing through a corner cube depends on the angle of incidence the ray makes with a normal to the front surface of the corner cube. The path length increases as the angle of incidence increases. Therefore, the path differences for the corner cube interferometer shown in Figure 6, page 19, will change faster than it normally would as the grating table rotates. Peck (9) has thoroughly analyzed the theory of the corner cube interferometer with regard to this effect. A study of his work shows that, neglecting higher order terms, the path difference for corner cubes mounted as shown in Figure 6 will be given by

$$\begin{aligned} \text{path difference} = & 2\left[2s \cos \beta + 2 \mu D \left(1 - \frac{1}{\mu^2}\right) - 2\mu' D' \left(1 - \frac{1}{\mu'^2}\right)\right. \\ & \left. + \frac{D}{4\mu} \left(1 - \frac{1}{\mu^2}\right) \alpha^4 - \frac{D'}{4\mu'} \left(1 - \frac{1}{\mu'^2}\right) \alpha'^4\right], \end{aligned} \quad (26)$$

where, in his notation,  $\mu$  is the refraction index of a corner cube,  $D$  is the depth of the corner cube, and  $\alpha$  is the angle of incidence in air that a ray makes with a normal to the front surface of the corner cube. The

primed and unprimed symbols in equation (26) distinguish the values for the two corner cubes. The factor of two (not given in Peck's equation) in front of the square bracket takes care of the fact that each corner cube is double-passed by the light beam in its arm of the interferometer. The first term inside the brackets, when multiplied by the two outside the brackets, is the usual path difference associated with rotation of the corner cubes through an angle of  $\beta$ . The second and third terms in equation (26) are independent of  $\alpha$  and contribute only a constant path difference. The fourth and fifth terms depend on  $\alpha$ , as do the higher order terms not shown. The higher order terms are neglected because their coefficients are much smaller, and thus their contribution is much smaller than the contribution from the terms retained. It should be noted that all terms, except the first terms, cancel out in pairs if the corner cubes are identical so that  $\mu = \mu'$  and  $D = D'$  and if the corner cubes are aligned so that  $\alpha = \alpha'$ . Then the path difference is strictly due to rotation of the corner cubes with the grating table. If the corner cubes are not identical and are not aligned so that  $\alpha = \alpha'$ , then the additional path difference due to all these inequalities can be estimated from the third and fourth terms in equation (26) after including the factor of two outside the square brackets in equation (26),

$$\text{additional path difference} = \frac{D}{2\mu} \left(1 - \frac{1}{\mu^2}\right) \alpha^4 - \frac{D'}{2\mu'} \left(1 - \frac{1}{\mu'^2}\right) \alpha'^4. \quad (27)$$

The estimate is first made assuming that the corner cubes are identical. Then  $D = D'$  and  $\mu = \mu'$ . Then equation (27) becomes

$$\text{additional path difference} = \frac{D}{2\mu} \left(1 - \frac{1}{\mu^2}\right) (\alpha^4 - \alpha'^4). \quad (28)$$

Equation (28) will be the unwanted change in path difference when the grating table has rotated through an angle of  $\alpha$  from the zero path difference position. The assumption is made that the front face of the unprimed corner cube is perpendicular to the light beam when the grating table is in the zero path difference position. Let  $\alpha' = \alpha - \Delta\alpha$  where  $\Delta\alpha$  may be on the order of a few degrees or may be quite small. Equation (28) can then be expressed as

$$\text{additional path difference} = \frac{D}{2\mu} \left(1 - \frac{1}{\mu^2}\right) [\alpha^4 - (\alpha - \Delta\alpha)^4]. \quad (29)$$

Expansion of  $(\alpha - \Delta\alpha)^4$  leaves

$$\begin{aligned} \text{additional path difference} = \frac{D}{4\mu} \left(1 - \frac{1}{\mu^2}\right) [4\alpha^3 \Delta\alpha \\ - 6\alpha^2 (\Delta\alpha)^2 + 4\alpha (\Delta\alpha)^3 - (\Delta\alpha)^4]. \end{aligned} \quad (30)$$

Estimates of the additional path difference are made using  $\Delta\alpha = 0.02$  radians (slightly more than one degree) for various value of  $\alpha$ . Then the additional path difference is used to find how many additional fringes will be seen. All the estimates are made using  $D = 3.0$  centimeters and  $\mu = 1.55$ . The results are given in Table 3. The values of  $\alpha$  to be used in equation (30) are chosen to be round decimal number for convenience. Each corresponding value in degrees of the angle  $\alpha$  is rounded to the nearest tenth of a degree since these values are only given to roughly indicate the size of the angle. The number of additional fringes is given to two significant digits.

The values in Table 3 were found assuming that  $D = D'$ ,  $\mu = \mu'$ , and  $\Delta\alpha = 0.02$  radians. Next the effect of not having identical corner cubes

TABLE 3

THE NUMBER OF ADDITIONAL FRINGES CAUSED BY MISALIGNMENT OF THE  
CORNER CUBES, FOR VARIOUS ANGULAR POSITIONS  
OF THE GRATING TABLE

radians	degrees	additional path difference cm x 10 <sup>-5</sup>	additional fringes
0.04	2.3	0.13	0.02
0.08	4.6	1.6	0.25
0.20	11.5	31	4.9
0.40	22.9	270	42

is estimated by assuming that  $D = 3.0$  cm.,  $D' = 2.8$  cm.,  $\mu = 1.55$ , and  $\mu' = 1.50$ . As in the case of identical corner cubes  $\alpha'$  is assumed to be less than  $\alpha$  by 0.02 radians. Equation (27) is used to get the additional path difference due to the fact that  $\mu \neq \mu'$  and  $D \neq D'$ . The results are shown in Table 4. The number of additional fringes seen is also given.

TABLE 4

THE NUMBER OF ADDITIONAL FRINGES CAUSED BY MISALIGNMENT OF THE  
CORNER CUBES AND BY NOT HAVING IDENTICAL CORNER CUBES,  
FOR VARIOUS ANGULAR POSITIONS OF THE GRATING TABLE

radians	degrees	additional path difference cm x 10 <sup>-5</sup>	additional fringes
0.08	4.6	1.6	0.25
0.20	11.5	55	8.7
0.40	22.9	480	75

A comparison of Table 4 with Table 3 shows that, for values of  $\alpha$  less than 4.6 degrees, the fact that  $\alpha \neq \alpha'$  and  $D \neq D'$  is not important. In fact, the effect was so slight that the results for 2.3 degrees are not shown. At larger values of  $\alpha$  the effect of not having identical corner cubes is as important as not having  $\alpha = \alpha'$ . For example, at 22.9 degrees about 33 more fringes are seen because  $\alpha \neq \alpha'$  and  $D \neq D'$ .

The additional fringes are seen in each case as the grating table turns from the zero path difference position to some value of  $\alpha$  associated with those additional fringes. For example, 8.7 additional fringes are seen as the grating tables turns from  $\alpha = 0$  to  $\alpha = 11.5$  degrees. The total number of fringes associated with this change in  $\alpha$  is about  $6.32 \times 10^5$ . Thus the error associated with detecting 8.7 more fringes is about one part in  $10^5$ --not a sizeable error at all. The error is of no importance when one considers the fact that the error is a systematic error which always affects the fringe occurrence in the same way each time.

## II. SINE DEPENDENCE OF THE FRINGE SPACING

The spacing of the fringes will be affected even more by the fact that path difference does not increase linearly with angle but as the sine of the angle from the zero path difference position. For example, consider the change in path difference produced by rotation of the grating table from an angular position of 4 degrees to an angular position of 5 degrees. The grating table must rotate through more than 1 degree when at 12 degrees to produce the same change in path difference. This effect will certainly affect the spacing of the markers. But this effect is

systematic and always affects the spacing the same way. Thus, the fringes and the markers derived from them will always occur at the same places, assuming such sources of erroneous fringe motion as temperature variation and vibration are not contributing noticeably of course. Since the spacing of the markers is affected in a repeatable fashion, the usefulness of the markers is not decreased. In fact, it is for this reason that no estimate is made of the effect of the sine dependence mentioned above.

## CHAPTER IX

### OPTICAL ALIGNMENT

The interferometer will be mounted as two separate units in the spectrometer. The beam splitter, the four plane front mirrors, and the detector will be mounted on the spectrometer table as one unit, and the corner cubes will be mounted on the grating table as the other unit. The position of the light source does not have to be inside the spectrometer tank and therefore may be chosen at some convenient point outside the tank.

Choose the position of the grating table to be associated with zero path difference. For the purposes for which this interferometer is intended, the zero path difference position will be with the grating oriented at the blaze angle. With the grating table in this position, note the line (represented by the dashed line AB in Figure 9) which passes through the position where the corner cubes are to be located. Figure 9 shows the same top view of the interferometer and grating table that was shown in Figure 6, page 19. Also, Figure 9 shows the beam splitter as having two faces--a more realistic picture of the beam splitter than that used in Figure 6. The same symbols are used to identify the optical components in Figure 9 that are used for them in Figure 6. The plane of the beam splitter should be oriented normal to line AB. The main reason for this is so that the optical layout will be symmetrical and will avoid unnecessary path differences. One face of the beam splitter is coated



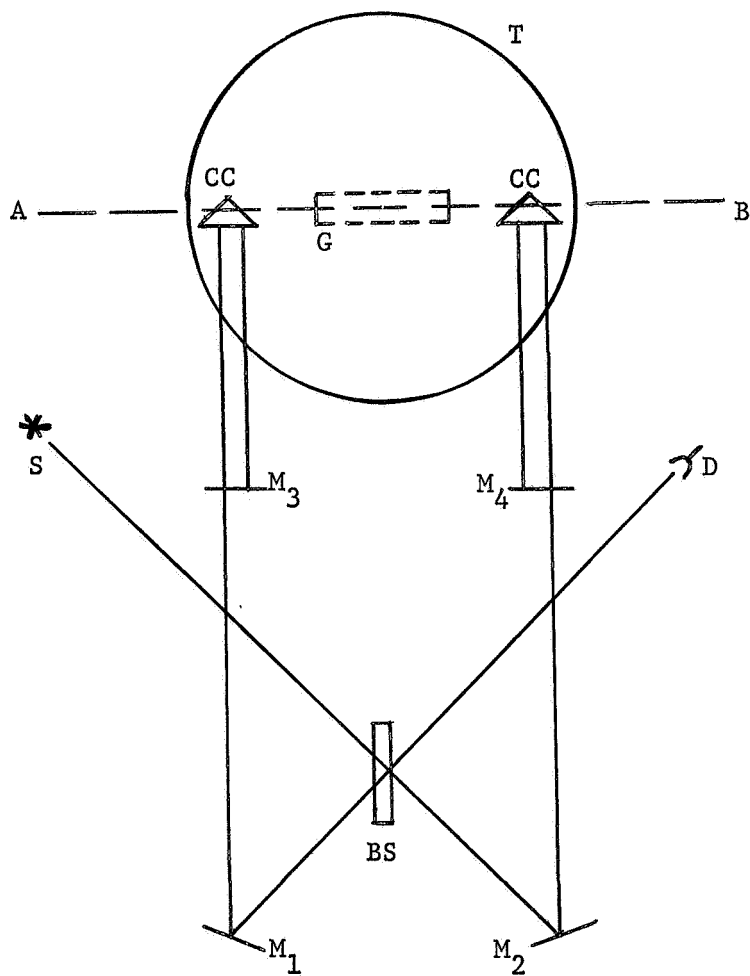


Figure 9. Top view of the optical layout of the Michelson interferometer.

with an antireflection coating so that most of the light passes through this side. Thus, most of the beam splitting occurs at the other face of the beam splitter; call it the primary face. Use an autocollimating telescope to make the normal of the primary face as horizontal as possible. (A horizontal laser may be used to make the normal of the primary face horizontal to a good approximation in a short time. Make the laser beam incident at about 45 degrees. Then adjust the beam splitter about its horizontal axis until the split beams are observed to be at the same height as the incoming beam. It should be noted that a laser beam can be made horizontal easily by using a mirror and an autocollimating telescope.)

The points where the beam-return mirrors  $M_3$  and  $M_4$  are placed should be chosen with reference to where the corner cubes are to be located when the grating table is in the zero path difference position. The mirrors  $M_3$  and  $M_4$  should be positioned so that the corner cubes can be rotated through their maximum range. The light beams coming from the corner cubes to these mirrors will "walk" across these mirrors as the corner cubes rotate with the grating table. Mirrors  $M_3$  and  $M_4$  are square so that the mirrors will offer more usable surface as the beams "walk" across them. Round mirrors would obviously not allow as much usable surface. The tops of the mirrors  $M_3$  and  $M_4$  should be lower than the top of the beam splitter by slightly less than one-half of the maximum beam displacement associated with the corner cubes so that the two beams from the beam splitter will pass over the tops of these mirrors. The displacement given to the beams by the corner cubes will bring the beams onto mirrors  $M_3$  and

$M_4$ . The two mirrors should be made coplanar to avoid any unnecessary path difference.

Ideally, it would be best to have mirrors  $M_1$  and  $M_2$  adjusted so that the divided beams travel exactly horizontal and parallel paths toward the corner cubes. Also, these parallel paths should be normal to a vertical plane passing through AB, as shown in Figure 9, page 46. Under these ideal conditions the interferometer is symmetrical, and the path difference results from rotation of the corner cubes with the grating table. This ideal situation is not necessary. Suppose mirrors  $M_1$  and  $M_2$  are aligned so that the divided beams do not follow parallel paths in going from  $M_1$  and  $M_2$  toward the corner cubes. Then mirrors  $M_3$  and  $M_4$  can be adjusted to make the beams retrace their paths as shown in Figure 10. Circular

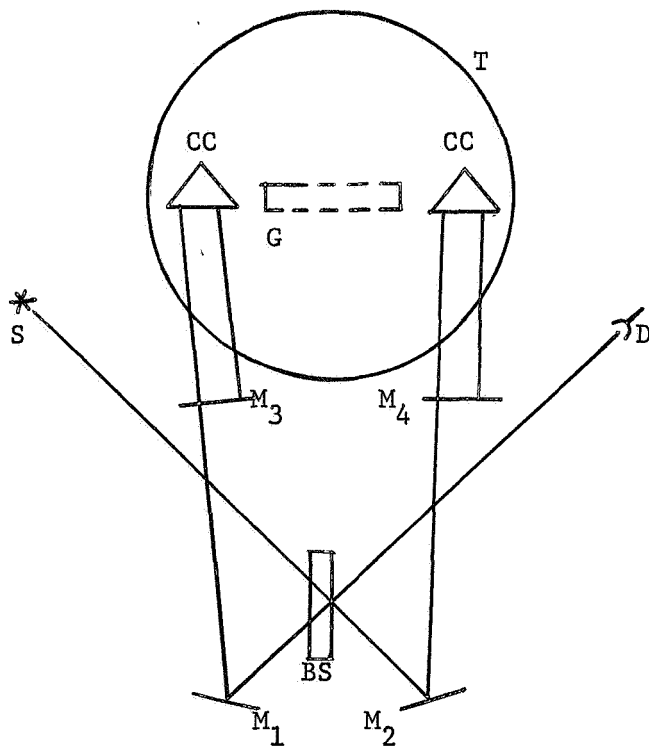


Figure 10. Asymmetric optical layout.

fringes will still be observed. An asymmetric optical layout introduces a small constant path difference which should be no problem since a laser source is used. Also, an asymmetric optical layout will decrease the maximum working angle of the interferometer. The beam in the left arm of the interferometer shown in Figure 9, page 46, will leave the corner cube at a smaller angle from the zero path difference position than the beam in the right arm which is aligned perpendicular to the vertical plane passing through AB. A minimal alignment effort, included in the alignment procedure given below, will reduce these effects.

Make a horizontal, unexpanded laser beam incident on the beam splitter at an angle of about 45 degrees. The normal of the primary surface of the beam splitter has previously been made horizontal. The beam will be split into two beams. Position  $M_1$  and  $M_2$  so that each mirror receives one of the split beams near its center. Turn mirrors  $M_1$  and  $M_2$  about their vertical and horizontal axes so that each directs the split beam toward where its associated corner cube will be located.

The next step, which can be omitted, is the minimal alignment effort referred to above. A test stand can be used to make the split beams both horizontal and parallel to a good approximation. This rigid test stand would be made with two holes at the same height above a reference level as the height of the original beam before it was split. The holes should be spaced the same distance apart as the separation of the beams just after they leave mirrors  $M_1$  and  $M_2$ . The hole size should be comparable to the size of the unexpanded laser beam in this region.

Next, place the corner cubes in position. The corner cubes are placed on the same diameter of the grating table at opposite sides of the grating. They should be positioned so that they are at about the same radial distance from the center of the table and on about the same diameter. However, an alignment effort to place the corner cubes at exactly the same radial position and exactly on the same diameter is not necessary because, as Marzolf (8) has shown, centering errors produce no interference effects. Marzolf aligns the corner cubes so that the corner lines appear superimposed when looking at the reflected images of the corner cubes from the position where the detector will be located. This should assure that the front faces of the corner cubes are very nearly parallel.

The split beams will be displaced downward and reflected toward mirrors  $M_3$  and  $M_4$ . Two red spots will be seen on  $M_1$  and two on  $M_2$ . One spot on each is the point where the split beam leaves to proceed toward its corner cube. The other spot on each mirror is where the split beams return. Adjust  $M_3$  and  $M_4$  so that the two spots on each mirror merge into one spot on each mirror. Some fine adjustment of  $M_1$  and  $M_2$  may also be necessary. When this merger occurs, the returning beams will coincide with the split beams heading toward their respective corner cubes, and circular fringes will be observed. Last of all, position the fringe detector so that it is centered in the central fringe.

## CHAPTER X

### SPECIFICATIONS OF COMPONENTS

The continuous helium-neon gas laser is an excellent source of light for interferometric work. It is a readily available, intense source of very nearly monochromatic light. Lasers which operate with only one longitudinal mode have a long coherence length which is desirable for a long path difference interferometer. The strong intensity of a laser source simplifies the problem of amplifying the detector output. A model 131 Spectra-Physics laser was used when the interferometer was set up.

The beam splitter is a rectangular plate, 1.5 x 1 x 3.8 inches, made of annealed BK7 glass. The front surface has a dielectric coating, and the back surface has a multilayer antireflection coating. These coatings were designed for a laser beam polarized normal to the plane of incidence. Transmission equals reflectance within 2-3 percent and absorption is less than 9.2 percent. The beam splitter mount provides fine adjustment of the beam splitter's position about a horizontal axis in its plane.

The four front surface mirrors are made of high quality borosilicate glass with a metallic coating. The front surface of each is flat to within one-fourth of the wavelength, and the reflectivity is 95 percent. Two of the mirrors ( $M_1$  and  $M_2$  in Figure 9, page 46) are round, and the diameter of each is 2.0 inches. The other two mirrors ( $M_3$  and  $M_4$  in Figure 9) are square, and the length of each side is 2.0 inches. The

mount for each mirror provides fine adjustment of the mirror's position about vertical and horizontal axes in the plane of the mirror.

The matched corner cubes are made of BK7 glass, and each has a 1.0 inch aperture. The edges of the corner cubes are knife-edged, rather than leveled, to reduce beam scatter by the edges. Total wave front distortion is less than one-tenth of a wavelength. Each corner cube provides 10 arc-second precision on the parallelism of beam return. The beam splitter, plane front mirrors, and corner cubes were obtained from Special Optics, Cedar Grove, New Jersey.

The detector is a field effect transistor packaged in a case with a glass lens top. The detector is used in the operational circuit shown in Figure 11. This circuit was suggested in the literature supplied with

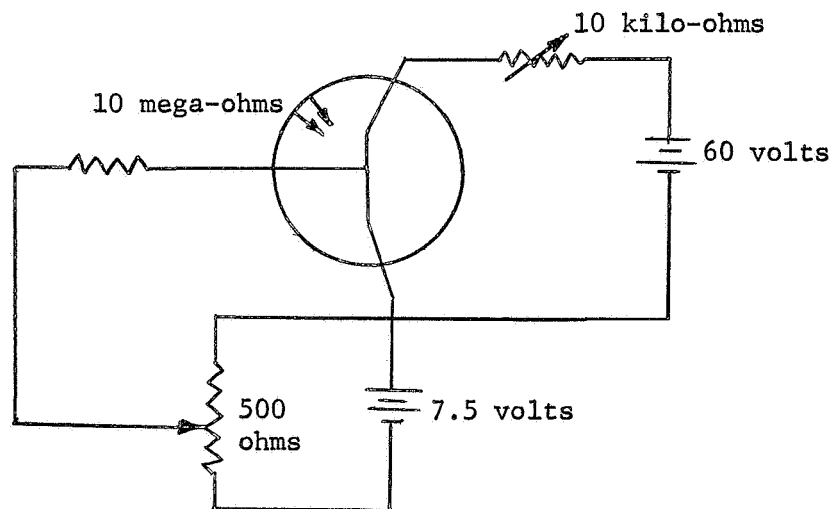


Figure 11. Operational circuit for the detector.

the detector by the manufacturer, Crystalonics, Cambridge, Massachusetts. A voltmeter placed across the 10 kilo-ohm variable resistor served as a meter. The voltage across this resistor will vary as the light intensity on the detector varies. This varying voltage can be used to provide the markers desired.



## CHAPTER XI

### SUGGESTIONS

The following suggestions are made for the use of the interferometer in the infrared spectrometer where it is to be placed. Some of these suggestions may be helpful for other applications of this interferometer.

A laser which has two or three longitudinal modes present might be tried first. This type of laser is not as expensive as a single longitudinal mode laser. If the maximum path difference allowed by visibility is not enough, then the single mode laser should be used. The light intensity of the laser chosen should be stable.

Try mounting the corner cubes on the grating table first. A special mount made of invar will be needed only if temperature fluctuations are a problem. If needed, the special mount will be difficult to place without interfering with the grating table. For this reason the special mount should be omitted, unless necessary.

A beam expander may be needed to remove the slight divergency of the laser beam and to make full use of the available optical aperture in the system. The beam expander should be mounted on the same base that the beam splitter is mounted on.

If variation of light intensity across the central fringe and variation of sensitivity across the detector are a problem, then a pair of optical stops and a lens should be used so that each point in

the central fringe is imaged at every point of the detector. First, a circular aperture stop would be placed in front of the detector. The diameter of this stop would be the smallest diameter which the central fringe will have. The smallest diameter will occur at the largest path difference. Then, a lens would be used to make the light coming through the aperture stop parallel. Then, another aperture stop would be placed at the exit pupil and the detector placed in this hole.

The following four steps are suggested for checking the interferometer:

Step 1. Record the detector output on chart paper when the detector is covered to keep out light. If the output varies, then there must be trouble in the detector or the circuitry following it. Repeat this step using another detector to see whether the detector or the circuitry is malfunctioning. Once this step is passed, proceed to step two.

Step 2. Use the detector and its associated circuitry to record the source intensity directly, before it enters the beam splitter, over a time period comparable to the longest scan time. If the value fluctuates, then the source intensity is varying. Note the frequency and magnitude of the fluctuation to determine if this fluctuation will affect the accuracy of line position measurements. After the system successfully passes this step, proceed to step three.

Step 3. Monitor the central fringe intensity with the grating table at rest for a time period comparable to the longest scan time. If the detector output varies, then there are several possible sources of error. If the frequency and amplitude of the fluctuation in detector

output are large enough to affect the accuracy of line position measurements, then these possible sources of error must be checked and eliminated if present. Monitor the spectrometer tank pressure to see if the air pressure is varying. Even this might not help because local outgassing in one arm of the interferometer could have a noticeable effect, and yet the tank pressure will appear to be stable. Temperature variation of the support for the corner cubes must be checked. The temperature at each location of a corner cube should be monitored by some remote means while the spectrometer tank is down to operating pressure. If the rate of temperature variation and the amplitude of the temperature variation are large enough to affect the accuracy of line position measurements, then an invar mount must be used for the corner cubes. If vibration of the optical components is suspected, then they should be insulated. Once the third step is passed, proceed to step four.

Step 4. Record the fringe detector output as a scan is made through known spectral lines from 2.5 degrees on one side of the zero path difference position to 2.5 degrees on the other side. Make the same scan again and check to see if the known lines have the same number of marker spaces between them. This will check the repeatability of the markers. If the markers are not repeatable, the grating table may be momentarily backing up. The regularity of the chart paper drive can be checked simultaneously in this step by recording an accurate time marker.

If the interferometer performs quite well, then perhaps in the future the interferometer may be made more sensitive by using more corner cubes as shown in Figure 12. This figure only shows the corner

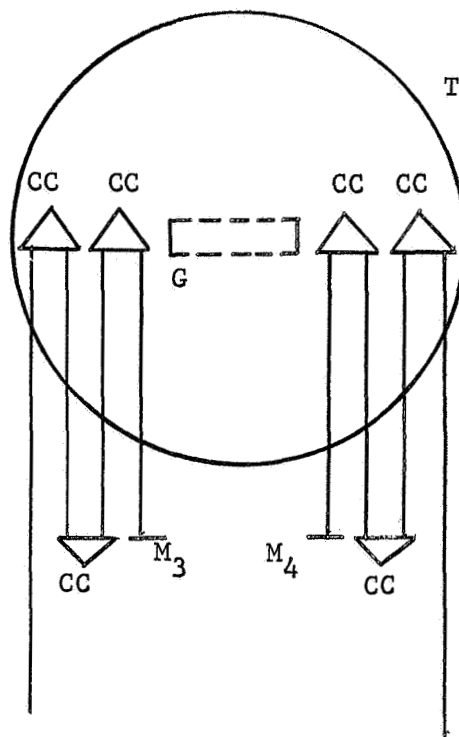


Figure 12. Possible future optical layout.

cubes mounted on the grating table and the corner cubes and front surface mirrors used for beam return. The remainder of the optical layout is the same as that shown in Figure 6, page 19. Such an optical layout may be difficult to achieve. In principle, the path difference when the table shown in Figure 12 is at an angle  $\theta$  from the zero path difference position would be on the order of  $16R \sin \theta$ , where  $R$  is a distance related to the radial distances of the corner cube pairs. Since the path difference for the arrangement in Figure 12 is approximately twice that of the arrangement shown in Figure 6, for the same angular position of the grating table in each case, the fringes should form and disappear about twice as often.

## BIBLIOGRAPHY

## BIBLIOGRAPHY

1. Ameer, George A. and William M. Benesch, *J. Opt. Soc. Am.*, 51, 303 (1961).
2. Rank, D. H., D. P. Eastman, W. B. Birtley, G. Skorinko, and T. A. Wiggins, *J. Opt. Soc. Am.*, 50, 821 (1960).
3. Rank, D. H., D. P. Eastman, B. S. Rao, and T. A. Wiggins, *J. Opt. Soc. Am.*, 51, 929 (1961).
4. Kuhn, H. G., E. L. Lewis, D. N. Stacey, and J. M. Vaughn, *Rev. Sci. Instr.*, 39, 86 (1968).
5. Gebbie, H. A., K. J. Habell, and S. P. Middleton, Proc. London Conference on Optical Instruments and Techniques (Chapman and Hall, Ltd., London, 1962), p. 43.
6. Sternberg, R. S. and J. F. James, *J. Sci. Instr.*, 41, 225 (1964).
7. Garing, J., Hdq. Air Force Cambridge Res. Lab. (OAR), L. G. Hanscomb Field, Bedford, Massachusetts (private communications).
8. Marzolf, J. G., *Rev. Sci. Instr.*, 35, 1212 (1964).
9. Peck, E. R., *J. Opt. Soc. Am.*, 38, 1015 (1948).
10. Cook, H. D. and L. A. Marzetta, *J. Res. Nat. Bur. Std.*, 65C, 129 (1961).
11. Peck, E. R. and S. W. Obetz, *J. Opt. Soc. Am.*, 43, 505 (1953).

## VITA

William L. Cole was born in [REDACTED] on [REDACTED] [REDACTED]

[REDACTED] He attended elementary and secondary public schools in Rockwood and entered The University of Tennessee at Knoxville, Tennessee, in September, 1957. In June, 1961, he received a B.S. degree in Engineering Physics from The University of Tennessee and entered the Graduate School at The University of Tennessee three months later.

The author is a member of Sigma Pi Sigma.